IRAS Studies of NO_2, N_2O_3, and N_2O_4 Adsorbed on Au(111) Surfaces and Reactions with Coadsorbed H_2O

Jiang Wang and Bruce E. Koel*

Department of Chemistry, University of Southern California, Los Angeles, California 90089-0482

Received: April 29, 1998; In Final Form: August 18, 1998

Adsorption or bonding geometries of pure adlayers of several N_xO_y species, i.e., nitrogen dioxide (NO_2), dinitrogen trioxide (N_2O_3), and dinitrogen tetroxide (N_2O_4), on Au(111) were determined by utilizing infrared reflection−absorption spectroscopy (IRAS). Dosing NO_2 on Au(111) at 85 K produced, in our experiments, mixtures of NO_2 and N_2O_3 (from contaminant NO) at submonolayer coverages and NO_2, N_2O_3, and N_2O_4 at monolayer coverages. However, a pure adlayer of chemisorbed NO_2 could be prepared by forming the monolayer on Au(111) at 85 K and then heating to 185 K or by NO_2 exposures on Au(111) at 185 K. Chemisorbed NO_2 is bonded to the surface in an O,O′-chelating geometry with C_{2v} symmetry. A monolayer of adsorbed N_2O_3 was produced by exposing the pure, chelating NO_2 adlayer to NO(g). The adsorbed complex with N_2O_3 has C_s symmetry, and we believe that N_2O_3 is bonded to the surface through one oxygen. Large NO_2 exposures can be used to produce crystalline N_2O_4 multilayers that have a preferential orientation of the N−N bond perpendicular to the Au(111) surface. To probe important aspects of the reactivity of these species with water and to investigate structure−reactivity relationships in this chemistry, we studied the reaction of each of these species with coadsorbed H_2O. Upon being heated, reactions proceed via two pathways. One route produces nitrous acid (HONO) and nitric acid (HNO_3) and occurs for all of the nitrogen oxide species listed above. These reactions do not depend on the degree of crystallinity of the condensed water clusters. A separate path occurs only for co-condensed amorphous ice clusters and multilayer N_2O_4 films, as signaled by the formation of oxygen adatoms on the Au(111) surface. These results reveal new information about fundamental interactions of nitrogen oxides and water in condensed phases.

Downloaded via PRINCETON UNIV on March 16, 2021 at 19:07:17 (UTC).
See https://pubs.acs.org/sharingguidelines for options on how to legitimately share published articles.

1. Introduction

Nitrogen oxides exhibit a wide variety of structures and have a rich chemistry.[1] Also, many different metastable N_xO_y intermediates[2] can be formed during reactions, and taken together, this has limited the understanding of the chemistry of nitrogen oxides and the development of structure−reactivity relationships. In particular, for interactions with metal atoms, a variety of bonding geometries are usually available. For example, NO_2 is well-known as a versatile linkage isomer in coordination compounds[3] and on metal surfaces.[4,5] However, we believe that it is possible to exploit this versatility to cleanly prepare and probe the condensed-phase chemistry of NO_2 and other nitrogen oxides by utilizing suitable substrates in surface-science-type experiments.

Au(111) surfaces are very unreactive and thus can be used in many cases to serve as an inert support for condensed phases. Recently, we have studied reactions after NO_2 exposures on ice films on Au(111).[6,7] We proposed that two separate reaction channels occur. One pathway forms nitrous acid (HONO) and nitric acid (HNO_3) and occurs for reactions of either amorphous or crystalline ice with NO_2, N_2O_3, and N_2O_4 at temperatures below 145 K. Another pathway ultimately forms oxygen adatoms on the Au(111) surface. In these reactions, we believe that Au(111) does not play a significant role in the nascent chemistry of $H_2O + NO_2$ but rather serves as an integrating detector for certain reaction products by decomposing those products at higher temperatures to produce surface oxygen. In this latter reaction channel, we observed two intermediates, the nitrito isomer of N_2O_4 (ONO−NO_2) and nitrosonium nitrate ($NO^+NO_3^-$), and we proposed that N_2O_4 was responsible for the formation of oxygen adatoms as shown in the following mechanism.[7]

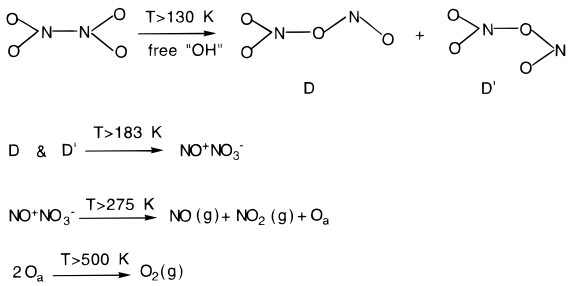

In these reactions, however, the specific reactivity of NO_2 or N_2O_3 with ice and their role in oxygen formation remains unclear. Use of a Au(111) substrate also allows us to address these issues. Previously, we have studied NO_2 adsorption on Au(111)[8] and Au(poly)[9] by HREELS and TPD and proposed methods to produce pure NO_2 and N_2O_3 monolayers on Au surfaces. Because we can separately form pure NO_2 and N_2O_3 monolayers on Au(111), we can better understand the individual reactivities of NO_2 and N_2O_3 with H_2O, as either amorphous or crystalline ice, by preadsorbing pure NO_2 and N_2O_3 monolayers on Au(111) and studying the subsequent surface reactions with postdosed water to form ice films.

* To whom correspondence should be addressed.

10.1021/jp982061d CCC: $15.00 © 1998 American Chemical Society
Published on Web 09/29/1998

This paper presents results of temperature-programmed desorption (TPD) and infrared reflection−absorption spectroscopy (IRAS) investigations of the composition and adsorption geometry of NO_2, N_2O_3, and N_2O_4 adlayers on Au(111). We also obtain new information on the reacting species in condensed films of $NO_2 + H_2O$ that lead to oxygen formation on the Au(111) surface. Pure N_2O_3 and chemisorbed, chelating NO_2 monolayers do not react with amorphous ice to form oxygen on Au(111). Only N_2O_4 multilayer films produce oxygen adatoms in these reactions, and the results are identical to those obtained by reacting N_2O_4 films on ice films pre-formed on the Au(111) surface. This further supports our proposal that formation of the nascent intermediates that lead to oxygen deposition on the Au(111) surface is not caused by the presence of the Au surface atoms but is caused by "free OH" groups on the amorphous ice surface.

2. Experimental Methods

The stainless steel ultra-high vacuum (UHV) chamber used in these experiments was pumped by a 240 L/s ion pump, a 240 L/s turbomolecular pump, and a titanium sublimation pump. The base pressure was typically 2×10^{-10} Torr. The UHV chamber was equipped with a double-pass cylindrical mirror analyzer (CMA) for Auger electron spectroscopy (AES), reverse-view four-grid optics for low-energy electron diffraction (LEED), a UTI 100 C quadrupole mass spectrometer (QMS) for temperature-programmed desorption (TPD), and gas-dosing facilities.

Infrared reflection−absorption spectroscopy (IRAS) studies were carried out in a reaction antechamber attached to the top of the surface analysis chamber by using a Mattson Galaxy 6020 FTIR spectrometer. Ar^+ ion sputtering was also performed in this antechamber. The IR beam from the interferometer was focused on the crystal at a grazing incidence angle of ∼86°. The reflected light along the specular direction was recollimated and focused onto a narrow-band, liquid nitrogen-cooled mercury cadmium telluride (MCT) detector. IR spectra were collected with the sample at 86 K using 8 cm^{-1} resolution and 1000 scans in a 4 min. period. Clean surface (background) spectra were acquired after annealing the crystal to 550 K to desorb adsorbates and quickly cooling to 86 K, and these were then subtracted from the adsorbate-covered surface spectra.

TPD experiments were carried out using a random flux shield over the end of the QMS, with the sample approximately 0.5 cm away from the entrance aperture and in the line-of-sight of the QMS ionizer. Two high-transparency screens, one biased at −55 V on the end of the ionizer cage and one at ground potential on the flux shield, were used to suppress the low-energy electron flux from the QMS.[10] The heating rate in TPD was 3.5 K/s.

The Au(111) crystal was mounted as reported before.[6,7] The sample could be cooled to 85 K using liquid nitrogen or resistively heated to 1100 K. The temperature was measured by a chromel−alumel thermocouple pressed firmly into a hole drilled into the side of the crystal. The Au(111) surface was cleaned by repeated sputtering−annealing cycles using 500 eV Ar^+ bombardment at 300 K followed by annealing to 973 K for 10 min. The cleanliness and structure of the surface were checked by AES and LEED.

NO, NO_2, and H_2O exposures were made by means of a directed molecular beam doser utilizing a microcapillary array. NO (Matheson, 99.9%) and NO_2 (Matheson, 99.9%) were used as received. Deionized water (H_2O) was used after degassing via several freeze−pump−thaw cycles. To minimize reactions of NO_2 in the doser gas lines, stainless steel and gold-plated gaskets were utilized and the entire dosing manifold gas line was initially passivated at ∼150 °C under NO_2 pressure for 30 min.

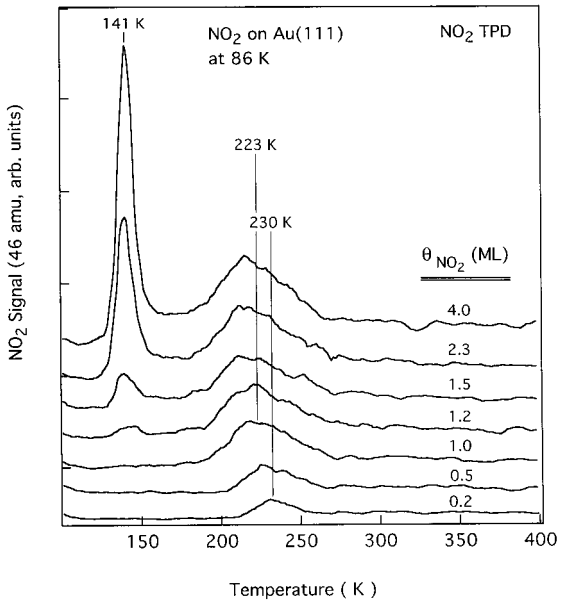

Figure 1. NO_2 TPD spectra following NO_2 exposures on Au(111) at 86 K.

Adsorbate coverages herein are referenced to $\Theta = 1$ ML for the saturation monolayer coverage of a given adsorbate on the Au(111) surface. NO_2 monolayer coverages were determined by TPD, referenced to saturation of the chemisorbed NO_2 peak at 220 K, which was defined as $\Theta_{NO_2} = 1$ ML (or 4.2×10^{14} molecules/cm^2).[8] The H_2O monolayer coverage was much less certain and was difficult to establish. Briefly, we used a background gas dose sufficient to adsorb one-half of the molecules required for the water bilayer (1.0×10^{15} molecules/cm^2) found on Pt(111)[11] assuming unit sticking probability.

3. Results and Discussion

3.1. Formation of Pure NO_2, N_2O_3, and N_2O_4 Adlayers on Au(111). Figure 1 shows TPD spectra for NO_2 desorption following NO_2 exposures on Au(111) at 86 K. NO_2 desorption initially occurs in a peak that shifts from 230 to 217 K with increasing coverage and then in a low-temperature peak at 141 K at higher exposures. This is consistent with earlier studies of NO_2/Au(111) that found completely reversible adsorption and assigned a peak at 223 K to desorption from the chemisorbed monolayer and a peak at 141 K to desorption from physisorbed N_2O_4 multilayers.[8,9,12] In Figure 1, we do not see any desorption at 325 K, which is an important feature in NO_2 TPD from Au(poly) surfaces,[9] indicating that our crystal had a negligible number of defects. The desorption activation energy for chemisorbed NO_2 was previously estimated to be 58 kJ/mol, and that for N_2O_4 multilayers was estimated to be 35 kJ/mol.[8]

Chemisorbed NO_2 on Au(111) has been assigned as an O,O′-nitrito surface chelate with C_{2v} symmetry based on HREELS.[8] Often, however, when working with HREELS resolutions of 80 cm^{-1} or so, there is a chance that overlapping peaks are not resolved and there is a small possibility that the loss peak at 1180 cm^{-1} in the work cited above could be due to two peaks of nearly the same energy arising from the asymmetric $\nu_a(NO_2)$ and symmetric $\nu_s(NO_2)$ NO_2 stretching modes. Interaction with the Au(111) surface could markedly decrease the energies of

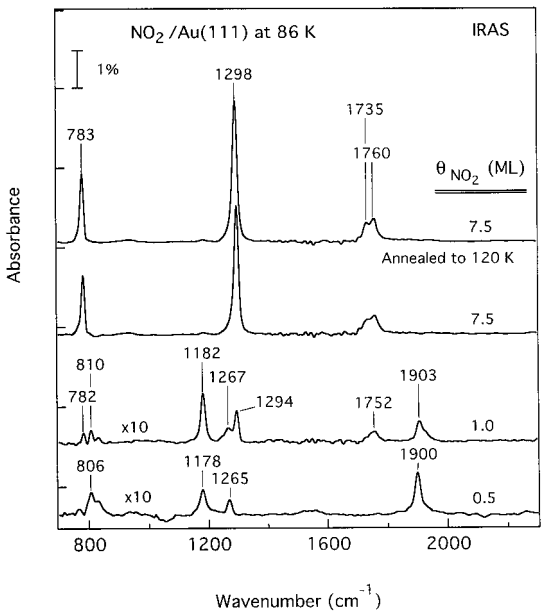

Figure 2. IRAS spectra after NO_2 exposures on a Au(111) surface at 86 K. All of the spectra were collected at 86 K.

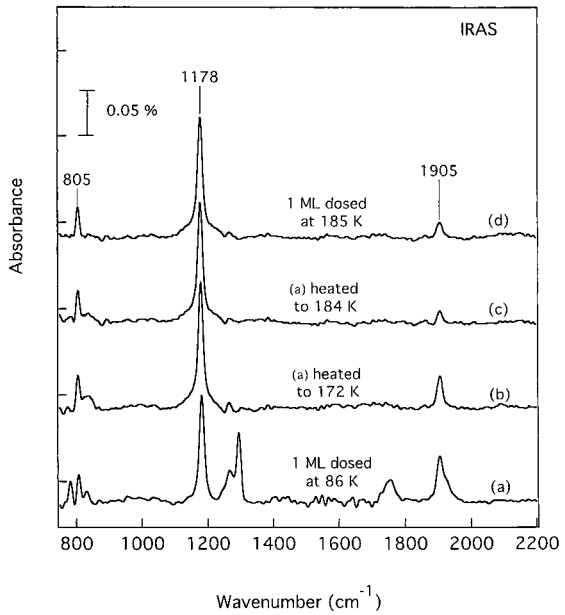

Figure 3. IRAS spectra obtained following: (a) 1 ML NO_2 dosed on Au(111) at 86 K; (b) annealing the surface in (a) to 172 K for 30 s; (c) annealing the surface in (a) to 184 K for 30 s; (d) dosing 1 ML NO_2 at 185 K. All of the spectra were collected at 86 K.

both of the $\nu_a(NO_2)$ and $\nu_s(NO_2)$ modes, which are 1618 and 1318 cm^{-1}, respectively in the NO_2 gas-phase IR spectrum.[13] For example, the NO_2 group in Ni(α-picoline)$_2$(NO$_2$)$_2$[14] has $\Delta[\nu_a(NO_2) - \nu_s(NO_2)] = 73$ cm^{-1}.

To better elucidate the adlayer composition and bonding geometry with increasing coverage and film thickness, we have obtained IRAS spectra of the adsorbed layers following NO_2 exposures on Au(111) at 86 K, as shown in Figure 2. Our assignments of these spectra are given in Table 1, and these agree with our previous HREELS data[8] very well. At 0.5 ML NO_2 coverage, a mixture of chemisorbed NO_2 and N_2O_3 exists on Au(111). N_2O_3 is formed by reaction of chemisorbed NO_2 with residual NO[8] in the background that arises from decomposition of NO_2 in the UHV chamber. Chemisorbed NO_2 has two peaks at 1178 and 806 cm^{-1} assigned previously to the symmetric stretching, $\nu_s(NO_2)$, and symmetric bending, $\delta(NO_2)$, modes, respectively, for a species bonded in an upright O,O′-chelating geometry with C_{2v} symmetry.[8] Two peaks due to N_2O_3 are seen at 1900 and 1265 cm^{-1} that arise from NO stretching, ν(NO), and NO_2 asymmetric stretching, $\nu_a(NO_2)$, modes, respectively. The other two peaks from N_2O_3 appear at 1178 and 806 cm^{-1} due to the $\nu_s(NO_2)$ and $\delta(NO_2)$ modes, which overlap with the same modes of chelating NO_2. At 1 ML NO_2 coverage, the adsorbed species are chelating NO_2, N_2O_3, and N_2O_4. The peaks at 1182 and 810 cm^{-1} are due to chemisorbed chelating NO_2. The peaks at 1903, 1267, 1182, and 810 cm^{-1} are from N_2O_3. The peaks at 1760, 1735, 1294, and 783 cm^{-1} are due to the $\nu_a(NO_2)$, $\nu_s(NO_2)$, and $\delta(NO_2)$ modes, respectively, of N_2O_4.[7,8,15,16] When the NO_2 coverage is 7.5 ML, only bands due to N_2O_4 were observed. Annealing this multilayer to 120 K does not change the IRAS spectra. This multilayer film can be described as pure crystalline N_2O_4 with a preferential orientation of the N−N bond almost perpendicular to the Au(111) surface, since it shows strong peaks due to $\nu_s(NO_2)$ modes along with fairly weak peaks due to $\nu_a(NO_2)$ modes.[15,16]

While the top two spectra in Figure 2 nicely characterize a condensed film with a pure N_2O_4 surface layer, we also wanted to obtain pure NO_2 and N_2O_3 layers. These were made by the procedure outlined in Bartram et al.,[8] and our IRAS spectra for chemisorbed NO_2 are shown in Figure 3. The pure, chemisorbed monolayer of NO_2 can be made by dosing NO_2 on Au(111) at 185 K or by dosing a NO_2 monolayer at 86 K and then heating to 185 K. Peaks at 1179 and 804 cm^{-1} are characteristic for chelating NO_2^- ligands in transition metal compounds.[3] As we have discussed for these compounds in more detail previously,[8] the $\delta(NO_2)$ mode is typically insensitive to the bonding geometry of NO_2, occurring at 817−863 cm^{-1}, but the $\nu_s(NO_2)$ mode is very sensitive to this bonding geometry. The $\nu_s(NO_2)$ mode has a frequency of 1171−1225 cm^{-1} for chelating isomers and 1306−1392 cm^{-1} for nitro isomers.[3,14,17] IRAS detects only one peak in the 1120−1220 cm^{-1} range that must be due to $\nu_s(NO_2)$ and no feature that can be assigned to $\nu_a(NO_2)$. Therefore, because of the strict dipole selection rule in IRAS (compared to HREELS) we show conclusively that chemisorbed NO_2 is bonded in an O,O′-chelating geometry with C_{2v} symmetry on Au(111), confirming the previous assignment made by using HREELS. The small peak at 1903 cm^{-1} is due

TABLE 1: Vibrational Frequencies (cm^{-1}) and Assignments of Adsorbed NO_2, N_2O_3, and N_2O_4 on Au(111) Surfaces

	NO_2/Au(111) NO_2 monolayer		N_2O_3/Au(111) N_2O_3 monolayer		N_2O_4/Au(111) N_2O_4 multilayer		
mode	HREELS[8]	IRAS	HREELS[8]	IRAS	HREELS[8]	IRAS[16]	IRAS
$\nu(O_2N-NO)$			250				
$\rho(O_2NNO)$			450−650		440		
$\delta_s(NO_2)$	800	805	800	806	770	785	783
$\nu_s(NO_2)$	1180	1178	1180	1182	1280	1301	1298
$\nu_a(NO_2)$	1180		1270	1272	1755	1750	1735, 1760
ν(NO)			1890	1897			

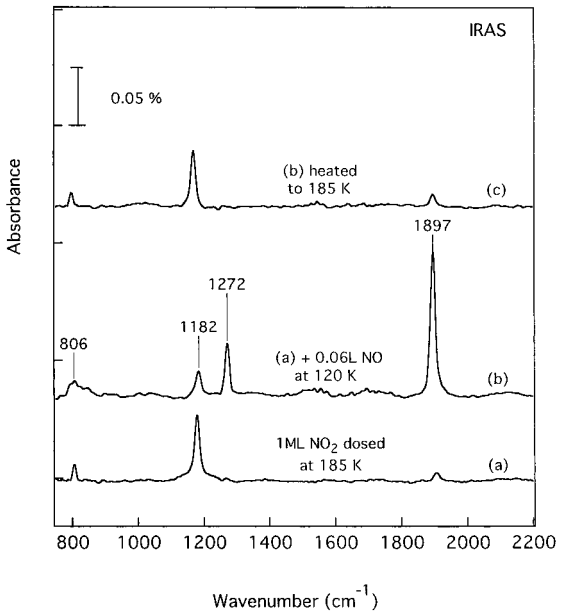

Figure 4. IRAS spectra obtained after (a) 1 ML NO_2 dosed on Au(111) at 185 K to give a pure monolayer of chelating chemisorbed NO_2, (b) NO exposure on a Au(111) surface precovered by the chelating NO_2 monolayer at 120 K to form a pure N_2O_3 monolayer, and (c) annealing the surface in (b) to 185 K for 30 s. All of the spectra were collected at 86 K.

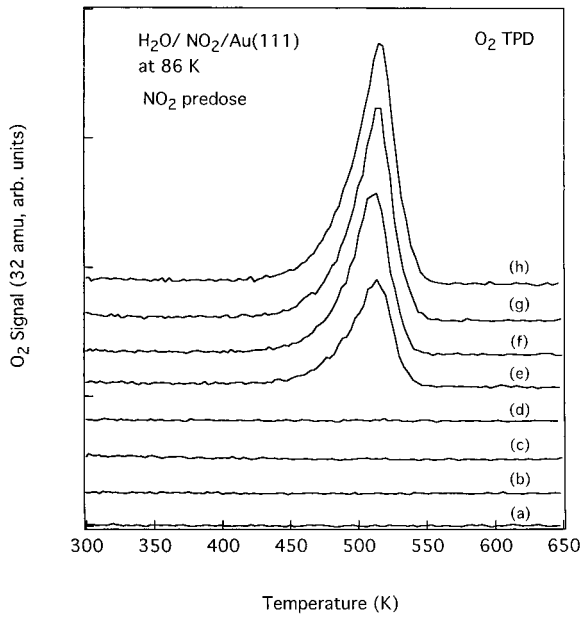

Figure 5. O_2 TPD spectra after predosing NO_2 on Au(111) at 86 K followed by H_2O exposures at the same temperature: (a) 1 ML H_2O dose after 0.5 ML NO_2; (b) 6 ML H_2O dose after 0.5 ML NO_2; (c) 0.5 ML H_2O dose after 1 ML NO_2; (d) 6 ML H_2O dose after 1 ML NO_2; (e) 1 ML H_2O dose after 5 ML NO_2; (f) 1 ML H_2O dose after 7.5 ML NO_2; (g) 4.5 ML H_2O dose after 7.5 ML NO_2; (h) 4.5 ML H_2O dose after 10 ML NO_2.

to the formation of a very small amount of N_2O_3 by reaction of residual NO in the chamber with chemisorbed NO_2.

A pure N_2O_3 monolayer can be readily made from the pure chelating NO_2 monolayer on Au(111) by NO exposure to the adlayer at 120 K. All of the peaks in the IRAS spectrum in Figure 4 can be assigned to N_2O_3. The strongest peak at 1898 cm^{-1} is due to the ν(N═O) mode, and the peaks at 1273, 1184, and 804 cm^{-1} are due to the $\nu_a(NO_2)$, $\nu_s(NO_2)$, and $\delta(NO_2)$ modes, respectively. We propose that adsorbed N_2O_3 is bonded to the surface with C_s symmetry using one oxygen atom, in a monodentate fashion, with its O_2NN═O bond perpendicular to the Au(111) surface. First, the $\nu_a(NO_2)$ and $\nu_s(NO_2)$ peaks have comparable intensity in the gas phase, and we observed comparable intensity of the $\nu_a(NO_2)$ and $\nu_s(NO_2)$ modes for the chemisorbed species. The surface dipole selection rule should strongly attenuate the $\nu_a(NO_2)$ peak if a chelating O,O′-geometry were formed, and this does not occur. The observation of IR intensity ratios of the other bands different from those in gas-phase N_2O_3[18] indicates that the adsorbed species is oriented and that this orientation is not with the molecular plane parallel with the surface. Furthermore, the very strong intensity of the ν(N═O) mode is consistent with this dynamic dipole nearly perpendicular to the surface. When this monodentate N_2O_3 adlayer is heated to 185 K, chelating NO_2 appears again on the surface following the breaking of the N−N bond in N_2O_3. This is consistent with an N−N bond dissociation energy of 42 kJ/mol.[8] We can now point out that the strong ν(N═O) peak of pure adsorbed N_2O_3 shows that the amount of N_2O_3 coadsorbed with chelating NO_2 in Figure 3 is very small indeed.

Since NO is not adsorbed on the Au(111) surface even at 105 K,[8] this reaction likely occurs via an Eley−Rideal mechanism.[19] Chelating NO_2 on the Au(111) surface may exist as a surface-bound radical, with an unpaired electron on the N atom (if the hybridization of the gas-phase molecule is maintained), and the radical−radical coupling reaction with NO (also a radical with the unpaired electron on the N atom) would readily occur. The following schematic illustrates the proposed bidentate NO_2 and monodentate N_2O_3 species formed on Au(111).

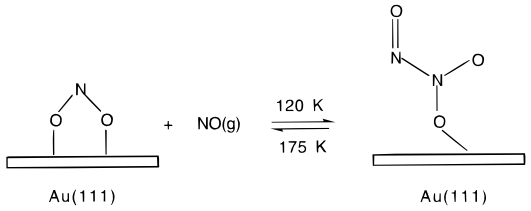

In all these IRAS studies, we did not observe any evidence for nitrite−N_2O_4 or $NO^+NO_3^-$ species formed from NO_2 exposures on Au(111). Koch et al.[16] did not observe these species either when they studied NO_2 adsorption on gold foil at 80 K.

3.2. Reactions of H_2O with Preadsorbed NO_2, N_2O_3, and N_2O_4 on Au(111). Water interacts very weakly with the Au(111) surface, TPD of H_2O on Au(111) does not resolve the desorption of any strongly bound, chemisorbed state, and no decomposition occurs.[7,20] Consistent with these reports, our TPD spectra show only a single narrow H_2O desorption peak, ranging from 153 to 165 K as the coverage increases.

Although NO_2 and H_2O adsorb molecularly and reversibly when adsorbed separately, coadsorption leads to reactions. Those reactions that lead ultimately to the deposition of oxygen adatoms on the surface are the easiest to monitor, because oxygen adatoms recombine on Au(111) and desorb as O_2 at 520−545 K leaving a clean surface.[21,22] Figure 5 shows O_2 TPD spectra that we used to monitor these reactions for a variety of coadsorption conditions. All of the exposures of both H_2O and NO_2 were carried out with the crystal at 86 K. The deposition of amorphous ice occurs at this low surface temperature.[7,23,24] O_2 desorption only results when the NO_2 preexposure was in the multilayer range forming a pure N_2O_4 film. The amount of oxygen formation saturates for NO_2 preexposures exceeding 10 ML. For NO_2 preexposures in the submonolayer range, forming a NO_2 and N_2O_3 precovered Au(111) surface, parts a and b of Figure 5 show that no oxygen was produced

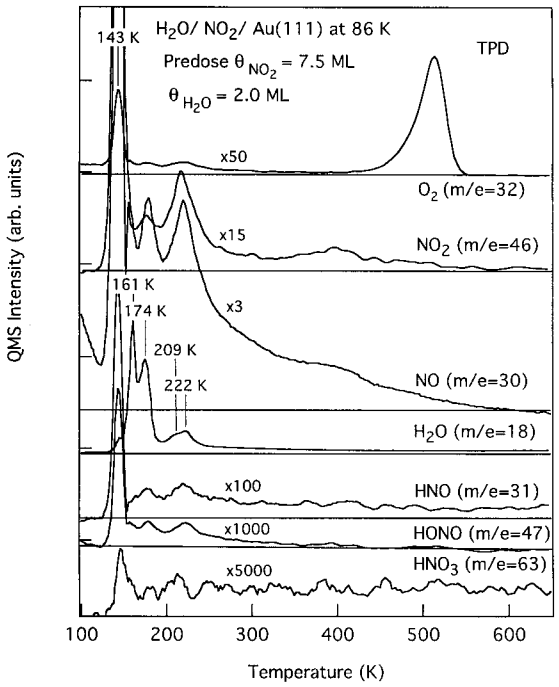

Figure 6. TPD spectra for several detected gas-phase products formed during heating in TPD after predosing 7.5 ML NO_2 on Au(111) at 86 K followed by a 2 ML H_2O exposure at the same temperature.

for 1−6 ML H_2O postdoses. This indicates that NO_2 and N_2O_3 are not responsible for oxygen formation. Moreover, parts c and d of Figure 5 show that no oxygen is produced when different postexposures of H_2O were dosed on the adlayer formed from a 1 ML NO_2 exposure on Au(111). This NO_2 dose forms a mixture of NO_2, N_2O_3, and N_2O_4 covering the surface. This result implies that interactions (hydrogen bonding) between N_2O_4 clusters and amorphous ice clusters are critical for oxygen deposition and coadsorbed NO_2 and N_2O_3 can block this interaction. These results are consistent with our observations that only N_2O_4 multilayer films react with amorphous ice clusters precovering the Au(111) surface and that the maximum amount of oxygen produced is about 0.5 ML.[6,7] This independence on the dosing sequence indicates that the Au surface plays little role in forming the initial intermediates that lead to oxygen formation and these are formed at the interface between N_2O_4 and amorphous ice.

Other products in addition to O_2 were liberated into the gas phase during heating in TPD after H_2O was exposed on an NO_2 precovered surface. For 2 ML H_2O exposed on a 7.5 ML NO_2 precovered Au(111) surface at 86 K, Figure 6 shows that signals in the QMS during TPD were observed at m/e = 63, 47, 31, 46, 30, 18, and 32. These masses ostensibly monitor HNO_3, HONO, HNO, NO_2, NO, H_2O, and O_2, respectively. No evidence was observed in TPD for other possible reduction products such as H_2, N_2, NH_3, N_2O, and NH_2NH_2. We propose that HONO and HNO_3 are produced from these coadsorbed layers under UHV conditions below 145 K. The gas-phase HNO_3 mass spectrum shows a parent peak (m/e = 63) that is only 1% in the mass spectrum cracking pattern, and HNO_3 does not produce HONO as an ion fragment.[25] It is uncertain whether HNO is a reaction product because the HONO mass spectrum is unknown and HNO could be a cracking fragment of HONO. In contrast to the oxygen formation pathway, acid formation reactions occur regardless of the NO_2 exposures, dosing sequence, or crystallinity of H_2O in the coadsorbed layer.

The reactions during TPD depicted in Figure 6 are very complicated, but we tentatively assign the peaks in the low-temperature range as follows. The peak at 161 K in H_2O TPD is assigned to unreacted water because the desorption temperature is the same as that of multilayer H_2O. The other three H_2O desorption peaks at 174, 209, and 222 K arise either from interactions of H_2O with adsorbed N_2O_4 or from cracking of higher molecular weight products. Since the gas-phase N_2O_4 mass spectrum does not give a fragment ion of m/e = 32, the peak at 143 K in O_2 TPD must be assigned to cracking from HNO_3 or HONO (or possibly some other unknown species). The O_2 peaks at 174, 209, and 222 K also arise from cracking of the products. In NO TPD, the peaks at 143, 174, and 222 K can be assigned to cracking from N_2O_4, HNO_3, and other products. The long "tailing" of the NO desorption trace with a peak at 350−430 K is unusual and is likely to indicate that the decomposition of intermediates that finally produce oxygen adatoms on Au(111) cause reaction-rate-limited NO desorption over a wide temperature range. In NO_2 TPD, the peak at 143 K is mainly due to cracking from unreacted N_2O_4 and the two higher desorption NO_2 peaks at 174 and 222 K arise from cracking of other products. In addition, the NO_2 TPD spectra also have a desorption profile that extends to quite high temperatures, including a peak at 350−430 K. This high-temperature NO_2 desorption is also reaction-rate limited[7] and is similarly produced from the decomposition of intermediates that finally generate oxygen adatoms on Au(111).

In other studies, we found that the oxygen formation reaction was highly dependent on the crystallinity of the ice when N_2O_4 reacts with ice films on Au(111).[6,7] Figure 7a shows that this phenomena was also observed in the experiments in which H_2O was exposed on N_2O_4 films. Figure 7a, trace iii, shows that a substantial amount of O_2 was produced in TPD when 7.5 ML NO_2 (pure N_2O_4) was predosed on a Au(111) followed by dosing 1 ML H_2O at 86 K. In Figure 7a, trace ii, a predosed 7.5 ML NO_2 film at 86 K was annealed to 115 K for 30 s and then 1 ML H_2O was dosed on the film at 86 K. Under the conditions of Figure 7a, trace ii, about the same amount of O_2 was produced as that in Figure 7a, trace iii. Consistently, IRAS shows in Figure 2 that the NO_2 multilayer formed on Au(111) at 86 K is pure N_2O_4 and subsequently annealing to 115 K does not change the chemical state of N_2O_4. In contrast, Figure 7a, trace i, shows that no O_2 was produced in TPD when a 7.5 ML NO_2 film was formed on Au(111) at 113 K and followed by dosing 1 ML H_2O on the Au(111) at 113 K. This result clearly demonstrates that the crystallinity of the deposited ice clusters is a crucial factor for oxygen formation.

Previous IRAS studies showed that amorphous ice was formed when H_2O was dosed on Au(111) at 86 K,[7] and this amorphous ice had non-hydrogen-bonded "free OH" groups.[23,26] These "free OH" groups were shown to have strong reactivity for oxygen formation when N_2O_4 reacts with preadsorbed ice films, and "free OH" groups also show greater reactivity in other reactions compared to fully hydrogen-bonded crystalline ice.[23,26,27] Annealing amorphous ice to 115 K or dosing H_2O at the same temperature produces crystalline ice and a loss in reactivity for oxygen formation since all of the "free OH" groups disappear because of crystallization that forms fully hydrogen-bonded ice species.[7,23,26] We propose that the strong hydrogen bonding between N_2O_4 and the highly polar "free OH" groups on the amorphous ice surface plays a crucial role in breaking the N−N bond (where $D(O_2N-NO_2)$ = 53 kJ/mol[8]) and stabilizing polar products and intermediates such as $ONO-NO_2$ and $NO^+NO_3^-$.

The reactivity of two other forms of nitrogen oxides, chelating chemisorbed NO_2 species and a pure monolayer of N_2O_3, with

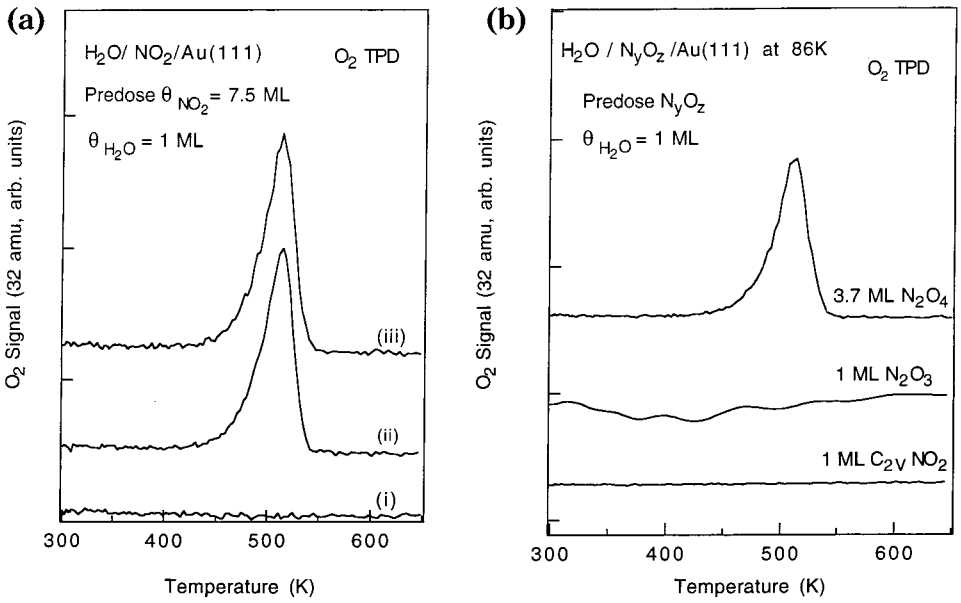

Figure 7. (a) O_2 TPD spectra probing requirements for generating surface oxygen: (i) 7.5 ML NO_2 predosed on Au(111) at 113 K followed by 1 ML H_2O exposure at the same temperature; (ii) 7.5 ML NO_2 predosed on Au(111) at 86 K, then annealed to 115 K for 30 s, followed by dosing 1 ML H_2O on the film at 86 K; (iii) 7.5 ML NO_2 predosed on Au(111) at 86 K followed by 1 ML H_2O exposure at the same temperature. (b) O_2 TPD spectra probing the extent of oxygen formation on Au(111) for the reaction of amorphous ice clusters formed by 1 ML H_2O exposures on preadsorbed films of (bottom) chelating NO_2 monolayer, (middle) N_2O_3 monolayer, and (top) N_2O_4 multilayer.

postdosed amorphous ice clusters on Au(111) at 86 K was also studied by TPD. The O_2 TPD spectra in Figure 7b show that no O_2 was produced either in reactions between chelating NO_2 or pure N_2O_3 and amorphous ice. Therefore, only N_2O_4 can react efficiently with amorphous ice to eventually oxidize the Au surface, and coadsorbed N_2O_3 and chelating NO_2 block the interaction of "free OH" groups with N_2O_4 to inhibit oxygen formation at low NO_2 exposures.

Comparing these results with our previous studies of N_2O_4 reacting with preadsorbed amorphous ice films,[7] we find exactly the same results—acid formation and oxygen formation occur via two separate reaction pathways proceeding under different conditions. Acid-forming reactions are sensitive to neither the NO_2 exposure nor the crystallinity of the ice, but oxygen formation occurs only when amorphous ice is available and NO_2 exposure is in the multilayer range (to form pure N_2O_4). This demonstrates that the same oxygen formation mechanism is operating independent of the dosing sequence of NO_2 and H_2O. We further proved in this study that N_2O_4 is the only nitrogen oxide (of those investigated) that can (ultimately) produce oxygen by reacting with amorphous ice. This represents strong support for our proposed mechanism in which N_2O_4 first isomerizes and forms $NO^+NO_3^-$, which finally decomposes at higher temperatures to form atomic oxygen on Au(111) during TPD.

Finally, the whole area of how N_xO_y interacts with water is important in the atmosphere. These studies reveal new information about fundamental interactions between N_xO_y and water (ice), for example, extending previous fundamental studies of N_2O_5 and ice.[28−30]

4. Conclusions

IRAS confirms the bonding geometries of NO_2, N_2O_3, and N_2O_4 adlayers on Au(111) deduced in previous HREELS studies. NO_2 exposures on Au(111) at 185 K produce a pure monolayer of chemisorbed, O,O′-chelating NO_2 with C_{2v} symmetry. Exposing this chemisorbed NO_2 monolayer on Au(111) at 120 K to gas-phase NO leads to a monolayer of adsorbed N_2O_3 that is bonded to the surface through one oxygen and has C_s symmetry. This conclusion about the monodentate bonding of N_2O_3 clarifies the ambiguity that was left in the previous HREELS determination. Large NO_2 exposures on Au(111) at 86 K produce crystalline N_2O_4 multilayers with a preferential orientation of the N−N bond perpendicular to the Au(111) surface.

Two reaction paths are found when preadsorbed layers of nitrogen oxides (NO_2, N_2O_3, and N_2O_4) on Au(111) react with ice clusters formed by postdosing H_2O on these surfaces at low temperatures. One path is associated with HONO and HNO_3 formation. This reaction channel proceeds regardless of the water exposure temperature (which controls the crystallinity and concentration of "free OH" groups of the ice clusters formed) and the size of the NO_2 exposures. The other reaction channel forms oxygen adatoms on the Au(111) surface during heating, and this pathway occurs only at the interface between amorphous ice clusters and N_2O_4 in films deposited on Au(111). Conditions that form crystalline ice strongly inhibit this reaction. Also, two other adsorbed nitrogen oxides species, i.e., chelating NO_2 and N_2O_3, that are normally observed following NO_2 exposures on Au(111) at 86 K cannot react with amorphous ice to form oxygen on Au(111). These results are consistent with those of our previous studies of nitrogen oxides from NO_2 exposures reacting with amorphous ice films predeposited on Au(111). These observations support our proposed mechanism for the formation of oxygen adatoms on Au(111) in which nitrite−N_2O_4, a reactive precursor, is formed by interactions between "free OH" groups of amorphous ice and N_2O_4 and then this species is converted to nitrosonium nitrate($NO^+NO_3^-$), which produces oxygen adatoms on the surface following thermal decomposition.

These facile reactions between N_xO_y and H_2O, along with the new structure−reactivity relationships established, are important to chemical foundations for a number of technologies, ranging from energetic materials to atmospheric chemistry.

Acknowledgment. This work was supported by the Army Research Office.

References and Notes

(1) Cotton, F. A.; Wilkinson, G. *Advanced Inorganic Chemistry*; Wiley-Interscience: New York, 1988.
(2) Hisatsune, I. C.; Devlin, J. P.; Wada, Y. *J. Chem. Phys.* **1960**, *33*, 714.
(3) Hitchman, M. A.; Rowbottom, G. L. *Coord. Chem. Rev.* **1982**, *42*, 55.
(4) Koel, B. E.; Bartram, M. E. *J. Vac. Sci. Technol.* **1988**, *A6*, 782.
(5) Koel, B. E. *Chemically Modified Oxide Surfaces*; Leyden, D. E., Collins, W. T., Eds.; Gordon and Breach Science Publishers: New York, 1989.
(6) Wang, J.; Voss, M. R.; Busse, H.; Koel, B. E. *J. Phys. Chem.* **1998**, *B102*, 4693.
(7) Wang, J.; Koel, B. E. *Surf. Sci.*, submitted.
(8) Bartram, M. E.; Koel, B. E. *Surf. Sci.* **1989**, *213*, 137.
(9) Wickham, D. T.; Banse, B. A.; Koel, B. E. *Catal. Lett.* **1990**, *6*, 163.
(10) Xu, C.; Koel, B. E. *Surf. Sci*. **1993**, *292*, L803.
(11) Wager, F. T.; Moylan, T. E. *Surf. Sci.* **1987**, *182*, 125.
(12) Bartram, M. E.; Windham, R. G.; Koel, B. E. *Surf. Sci.* **1987**, *57*, 184.
(13) Arakawa, E. T.; Nielsen, A. H. *J. Mol. Spectrosc*. **1958**, *2*, 413.
(14) Goodgame, D. M. L.; Hitchman, M. A. *Inorg. Chem*. **1965**, *4*, 721.
(15) Sjovall, P.; So, S. K.; Kasemo, B.; Franchy, R.; Ho, W. *Chem. Phys. Lett.* **1990**, *171*, 125.
(16) Koch, T. G.; Horn, A. B.; Chesters, M. A.; McCoustra, M. R. S.; Sodeau, J. R. *J. Phys. Chem.* **1995**, *99*, 8362.
(17) Nakamoto, K. *Infrared and Raman Spectra of Inorganic and Coordination Compounds*; Wiley: New York, 1986.
(18) Bibart, C. H.; Ewing, G. E. *J. Chem. Phys.* **1974**, *61*, 1293.
(19) Somorjai, G. A. *Interoduction to Surface Chemistry and Catalysis*; John Wiley & Sons Inc.: New York, 1994.
(20) Kay, B. D.; Lykke, K. R.; Creighton, J. R.; Ward, S. J. *J. Chem. Phys*. **1989**, *91*, 5120.
(21) Parker, D. H.; Koel, B. E. *J. Vac. Sci. Technol.* **1990**, *A8* (3), 2585.
(22) Saliba, N.; Parker, D. H.; Koel, B. E. *Surf. Sci*., in press.
(23) Schaff, J. E.; Roberts, J. T. *J. Phys. Chem.* **1994**, *98*, 6900.
(24) Buch, V.; Devlin, J. P. *J. Chem. Phys.* **1991**, *94*, 4091.
(25) Dohl-oelze, R.; Brown, C. C.; Stuve, E. M. *Surf. Sci.* **1989**, *210*, 339.
(26) Rowland, B.; Fisher, M.; Devlin, J. P. *J. Phys. Chem.* **1993**, *97*, 2485.
(27) Gertner, B. J.; Hynes, J. T. *Science* **1996**, *271*, 1563.
(28) Tolbert, M. A.; Rossi, M. J.; Golden, D. M. *Science* **1988**, *240*, 1018.
(29) Chu, L. T.; Leu, M. T.; Keyser, L. F. *J. Phys. Chem.* **1993**, *97*, 12798.
(30) Finlayson-Pitts, B. J. *Atmospheric Chemistry: fundamentals and experimental techniques*; Wiley: New York, 1986.